

Fermi-liquid state in T^* -type $\text{La}_{1-x/2}\text{Eu}_{1-x/2}\text{Sr}_x\text{CuO}_4$ revealed via element substitution effects on magnetism

Takanori Taniguchi,^{1,*} Kota Kudo,^{2,1} Shun Asano,^{2,1} Motofumi Takahama,^{2,1} Isao Watanabe,^{3,†} Akihiro Koda,⁴ and Masaki Fujita^{1,‡}

¹*Institute for Materials Research, Tohoku University, Katahira, Sendai 980-8577, Japan*

²*Department of Physics, Tohoku University, Aoba, Sendai 980-8578, Japan*

³*Meson Science Laboratory, RIKEN Nishina Center for Accelerator-Based Science, RIKEN, Wako, Saitama 351-0198, Japan*

⁴*Institute of Materials Structure Science, High Energy Accelerator Research Organization, Tsukuba, Ibaraki 305-0801, Japan*

(Dated: August 9, 2024)

Despite its unique structural features, the magnetism of single-layered cuprate with five oxygen coordination (T^* -type structure) has not been investigated thus far. Here, we report the results of muon spin relaxation and magnetic susceptibility measurements to elucidate the magnetism of T^* -type $\text{La}_{1-x/2}\text{Eu}_{1-x/2}\text{Sr}_x\text{CuO}_4$ (LESCO) via magnetic Fe- and non-magnetic Zn-substitution. We clarified the inducement of the spin-glass (SG)-like magnetically ordered state in $\text{La}_{1-x/2}\text{Eu}_{1-x/2}\text{Sr}_x\text{Cu}_y\text{Fe}_{1-y}\text{O}_4$ with $x = 0.24 + y$, and the non-magnetic state in $\text{La}_{1-x/2}\text{Eu}_{1-x/2}\text{Sr}_x\text{Cu}_y\text{Zn}_{1-y}\text{O}_4$ with $x = 0.24$ after the suppression of superconductivity for $y \geq 0.025$. The SG state lies below ~ 7 K in a wide Sr concentration range between 0.19 and 0.34 in 5% Fe-substituted LESCO. The short-range SG state is consistent with that originating from the Ruderman-Kittel-Kasuya-Yosida interaction in a metallic state. Thus, the results provide the first evidence for Fermi liquid (FL) state in the pristine T^* -type LESCO. Taking into account the results of an oxygen K -edge X-ray absorption spectroscopy measurement [J. Phys. Soc. Jpn. **89**, 075002 (2020)] reporting the actual hole concentrations in LESCO, our results demonstrate the existence of the FL state in a lower hole-concentration region, compared to that in T -type $\text{La}_{2-x}\text{Sr}_x\text{CuO}_4$. The emergence of the FL state in a lower hole-concentration region is possibly associated with a smaller charge transfer gap energy in the parent material with five oxygen coordination.

PACS numbers: 74.25.Ha, 74.62.Bf, 74.72.-h, 76.75.+i

I. INTRODUCTION

A recent study on superconductivity in the $RE_2\text{CuO}_4$ (RE = rare earth) family has reported a variety of ground states due to different oxygen coordination around Cu^{2+} [1, 2]. It is well known that T -type La_2CuO_4 with six coordination is a Mott insulator that exhibits superconductivity with hole doping. T' -type $RE_2\text{CuO}_4$ with four planar coordination has also been considered to be the parent Mott insulator of electron-doped superconductors [3–6]. However, Yamamoto et al. reported the emergence of superconductivity in a thin film of T' -type $RE_2\text{CuO}_4$ [7–9], leading to the study of the actual ground state in $RE_2\text{CuO}_4$ with different coordinations [10, 11]. A theoretical study demonstrated a decrease in the electron correlation strength with increasing distance between the apical oxygen and the CuO_2 plane, supporting the metallic nature in T' -type cuprates [12]. In real materials, partially existing apical oxygen atoms in the as-sintered (AS) T' -type compounds are considered to inhibit superconductivity, owing to the introduction of a random electronic potential on the CuO_2 plane [13–15]. Thus, a reduction annealing procedure is necessary for the complete removal of excess oxygen to induce superconductivity [16].

In another structural isomer of $RE_2\text{CuO}_4$ with five coordination (T^* -type structure), superconductivity appears with hole doping and post annealing [17, 18]. T^* -type cuprates have an intermediate crystal structure be-

tween the T and T' -type cuprates, which contains a CuO_5 pyramid in the unit cell. Although studies on the physical properties of T^* -type cuprates is limited, Kojima et al. reported weak magnetism in T^* -type La_2CuO_4 [19], which is qualitatively similar to that in superconducting (SC) T' -type $RE_2\text{CuO}_4$ [19–21]. Thus, T^* -type cuprates are a notable system for studying the relationship between physical properties and oxygen coordination. However, owing to the limited availability of high-quality samples [22, 23], T^* -type cuprates have not been studied thoroughly.

Recently, we reported a magnetic and SC phase diagram of T^* -type $\text{La}_{1-x/2}\text{Eu}_{1-x/2}\text{Sr}_x\text{CuO}_4$ (LESCO) with x ranging from 0.14 to 0.26 by muon spin relaxation (μSR), magnetic susceptibility, and electrical resistivity measurements [24, 25]. All the AS and oxidation annealed (OA) samples in this x range exhibit magnetic order (spin-glass (SG) like state) and superconductivity, respectively. Therefore, the ground state varied drastically, and the metallic nature was markedly enhanced by annealing [25]. Furthermore, from the phase diagram against the actual hole concentration (p) estimated by O K -edge X-ray absorption spectroscopy, we clarified the increase in the SC transition temperature (T_c (onset)) with decreasing p for $0.09 \leq p \leq 0.17$ [26]. This result is different from the phase diagram of $\text{La}_{2-x}\text{Sr}_x\text{CuO}_4$ (LSCO), where the optimum p is ~ 0.16 [27]. SC states with higher T_c are achieved in the lightly doped region with $p \lesssim 0.09$, similar to the SC phase diagram of hole-

doped T' -type $\text{La}_{1.8-x}\text{Eu}_{0.2}(\text{Sr}, \text{Ca})_x\text{CuO}_4$ [11, 28, 29]. Thus, it is important to clarify the electronic state of LESCO in superconducting T^* -type RE_2CuO_4 .

Electronic states in pristine cuprates have been studied intensively through impurity substitution effects on magnetic correlations [30–40]. In LESCO, nonmagnetic Zn (Zn^{2+} , $S = 0$) substitution effectively enhances the magnetic order in the pristine sample with $p \lesssim 0.14$, and induces weak static magnetism, even for $p \gtrsim 0.14$ [31–33]. In addition, the substitution of magnetic impurity Fe (Fe^{3+} , $S = 5/2$) strongly stabilizes the magnetic order (SG-like state) over the entire SC phase [34–37]. It is worth noting that the magnetic properties stabilized in the underdoped (UD) and overdoped (OD) regions are different. Long-range and short-range magnetic orders are realized in the UD and OD regions, respectively, of Fe-substituted LESCO (Fe-LESCO) [37, 38]. Furthermore, a complementary study with angle-resolved photoemission and neutron scattering measurements revealed that the spin-density-wave order in OD Fe-substituted LSCO (Fe-LSCO) originates from the Fermi surface inherent in pristine LSCO. In contrast, the localized spins form a one-dimensional stripe-like domain in UD LSCO [35]. From these results, a doping-induced cross-over of the electronic state from the strongly correlated electronic state to the Fermi liquid (FL) state has been discussed [35, 39].

Following previous works [30–40], we investigated the magnetism in Fe-substituted LESCO (Fe-LESCO) and Zn-substituted LESCO (Zn-LESCO) by μSR and magnetic susceptibility measurements. This paper is organized as follows. We show the experimental procedures and the sample characterizations in Sect. 2 and Sect. 3A, respectively. The results of magnetization and μSR measurements are presented in Sect. 3B, and the interpretations are described in Sect. 3C. Our results elucidate the electronic state in superconducting T^* -type cuprates. To the best of our knowledge, this is the first study on the element substitution effect on magnetism in T^* -type cuprates.

II. SAMPLE PREPARATION AND EXPERIMENTAL DETAILS

Polycrystals of $\text{La}_{1-x/2}\text{Eu}_{1-x/2}\text{Sr}_x\text{Cu}_{1-y}(\text{Zn}, \text{Fe})_y\text{O}_4$ with $0.14 \leq x \leq 0.34$ and $0.025 \leq y \leq 0.10$ were prepared by an ordinary solid-state reaction method from pre-fired powders of La_2O_3 , Eu_2O_3 , SrCO_3 , Fe_2O_3 , ZnO , and CuO . As in Fe-LSCO, we introduced an additional Sr^{2+} ion to compensate for the reduction of p , by substituting Fe^{3+} into the Cu^{2+} site [42]. The value of additionally doped Sr is given by y [39, 41]. Since the actual p in LESCO is smaller than x , p in $\text{La}_{1-(x+y)/2}\text{Eu}_{1-(x+y)/2}\text{Sr}_x\text{Cu}_{1-y}\text{Fe}_y\text{O}_4$ may shift to the lower doping side with increasing y . However, this situation does not defeat the purpose of investigating the electronic state. The mixture of powders was pressed into

pellets, and sintered at 1050 °C in air with intermittent grinding, then annealed in oxygen gas at 40 MPa at 500 °C for 80 h to obtain OA samples. All samples used in the present study were OA samples. Magnetic susceptibility measurements were carried out under a magnetic field of 500 Oe, using a SC quantum interference device magnetometer (Quantum Design MPMS) to investigate the magnetism in Fe-LESCO and Zn-LESCO. In addition, to visualize the evidence of superconductivity in lightly Fe-substituted LESCO, the shielding and Meissner signals were measured under a field of 10 Oe. In our oxygen K -edge X-ray absorption spectroscopy, the carrier change, that occurs when Eu^{3+} is converted to Eu^{2+} , was not observed in LESCO. Therefore, Eu^{2+} does not contribute to the magnetism of LESCO [26].

We performed zero-field (ZF) μSR measurements using a pulsed positive muon beam on the S1 spectrometers in the Materials and Life Science Experimental Facility (MLF) in J-PARC, Japan, and a spectrometer (CHRONUS) at Port 4 in the RIKEN-RAL Muon Facility (RAL) in the Rutherford Appleton Laboratory, UK. Four pellets with a radius of 15 mm were prepared. Then, considering the beam size with a radius of 10–15 mm, the four pieces were cut into fan shapes to maximize the sample surface area while minimizing the beam hitting anything other than the sample. These four fan-shaped pieces were then arranged in a clover shape on a silver plate. All the Zn-LESCO, and a part of the Fe-LESCO with $x = 0, 24$ and $y = 0.05$ were measured at MLF. μSR is a powerful probe for the study of local magnetism, even in samples that are available only in powder form. The asymmetry parameter $A(t)$ (μSR time spectrum) given by $[F(t) - \alpha B(t)]/[F(t) + \alpha B(t)]$, where $F(t)$ and $B(t)$ are the total muon events at time t of the forward and backward counters located in the beamline, respectively, was measured. We denote the $A(t)$ normalized by the initial asymmetry $A(t = 0)$ after correcting the counting efficiencies as α . In this paper, we show the normalized time spectra after subtracting the background (BG). Since we observed the spectrum over a long time range, we estimated the constant BG in each Fe-doped sample so that the BGs of the spectra at the characteristic temperatures, that is, high temperature, low temperature, and near spin glass temperature become the same as each other. Then, the temperature-independent BG was subtracted from all the data.

III. RESULTS AND DISCUSSION

A. Characterization of samples

Since there are no studies regarding the element substitution of Cu sites in T^* -type cuprates, we first examined the structural aspect of the samples. Figures 1 (a) and (b) show the x-ray powder diffraction patterns of Fe-LESCO with $x = 0.14 + y$ and $0.24 + y$, and Zn-LESCO with $x = 0.14$ and 0.24 , respectively, for $0 \leq y \leq 0.10$. Fe

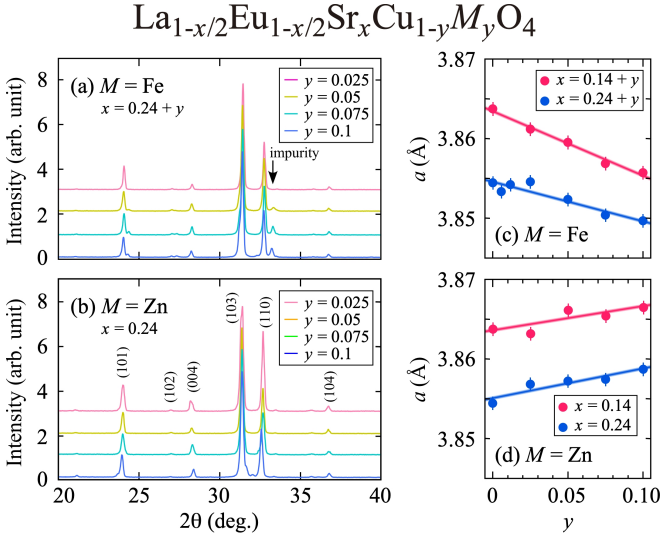


FIG. 1. (Color online) XRD pattern and in-plane lattice constant of (a), (c) Fe and (b), (d) Zn-substituted $\text{La}_{1-x/2}\text{Eu}_{1-x/2}\text{Sr}_x\text{Cu}_{1-y}\text{M}_y\text{O}_4$ with $x = 0.14 + y$, $x = 0.24 + y$, $x = 0.14$ and $x = 0.24$, respectively.

substitution tends to induce the little amount of the T' -type phase as the secondary phase, and the sample with $y \geq 0.075$ contains $\sim 5\%$ T' -type phase. All the samples of Zn-LESCO were confirmed to be a single phase of T^* -type cuprates. We evaluated the in-plane lattice constant (a) by Rietveld analysis of the diffraction pattern. The results are plotted in Figs. 1 (c) and (d) as a function of y . The shrinkage (elongation) of the a -axis with increasing y in Fe-LESCO (Zn-LESCO) is caused by replacing Cu^{2+} with Fe^{3+} (Zn^{2+}) having a smaller (larger) ionic radius than that of Cu^{2+} . Accordingly, the linear variation of the lattice constant suggests that the substitution has been almost achieved, although the impurity phase tends to appear in Fe-LESCO with increasing y .

B. Fe and Zn-concentration dependence of magnetism in $\text{La}_{1-x/2}\text{Eu}_{1-x/2}\text{Sr}_x\text{Cu}_{1-y}\text{M}_y\text{O}_4$

1. Magnetic susceptibility measurements

First, we examined the effects of Fe- and Zn substitution on the magnetism in LESCO with $x = 0.24$ ($p \sim 0.16$, $T_c = 11.9$ K). Figs. 2 (a) and (b) respectively show the temperature dependence of the magnetic susceptibility $\chi(T)$ for Fe-LESCO with $x = 0.24 + y$, and Zn-LESCO with $x = 0.24$ for $y = 0, 0.006, 0.012, 0.025, 0.050, 0.075$ and 0.10 . In Fe-LESCO, $\chi(T)$ measured after zero-field-cooling (ZFC) and field-cooling (FC) processes ($\chi(T)_{\text{ZFC}}$ and $\chi(T)_{\text{FC}}$, respectively) exhibits distinct behavior at low temperatures, suggesting the appearance of SG-like magnetic state by Fe-substitution. The T_{sg} where the $\chi(T)_{\text{ZFC}}$ exhibits a local maximum

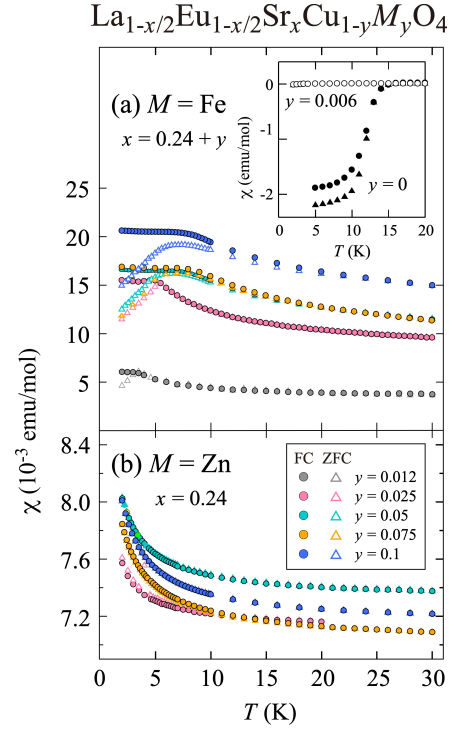


FIG. 2. (Color online) (a) Fe- and (b) Zn concentration dependence of magnetic susceptibility measured after zero-field and field-cooling processes for $\text{La}_{1-x/2}\text{Eu}_{1-x/2}\text{Sr}_x\text{Cu}_{1-y}\text{M}_y\text{O}_4$ with $x = 0.24 + y$ for Fe substitution, and $x = 0.24$ for Zn substitution.

slightly increases, and the cusp in $\chi(T)_{\text{ZFC}}$ for $y = 0.025$ turns into a broad peak for $y \geq 0.05$. The broadening of the cusp suggests the enhancement of magnetic defects for larger y . In Zn-LESCO, a paramagnetic behavior exhibiting an increase in $\chi(T)$ upon cooling was observed. Therefore, the magnetic ground state of Fe-LESCO and Zn-LESCO are different. The inset of Fig. 2 (a) indicates $\chi(T)_{\text{ZFC}}$ for Fe-LESCO with $x = 0.24 + y$ and $y = 0$ and 0.006 . The result for the pristine LESCO ($y = 0$) is taken from Ref. 25. Superconductivity is suppressed by the substitution of small amounts of Fe, following the emergence of the SG state.

2. μSR measurements

Here, we present the results of the μSR experiments. Figure 3 shows the μSR time spectra for Fe-LESCO with $(x, y) =$ (a) (0.265, 0.025), (b) (0.29, 0.050), and Zn-LESCO with $(x, y) =$ (c) (0.24, 0.025) and (d) (0.24, 0.050). In Fe-LESCO, the Gaussian-shaped spectra transformed into an exponential-shaped spectra upon decreasing the temperature, followed by the appearance of the fast depolarization component or oscillation component at low temperatures. A negligible temperature dependence of the Gaussian-shaped depolarization below

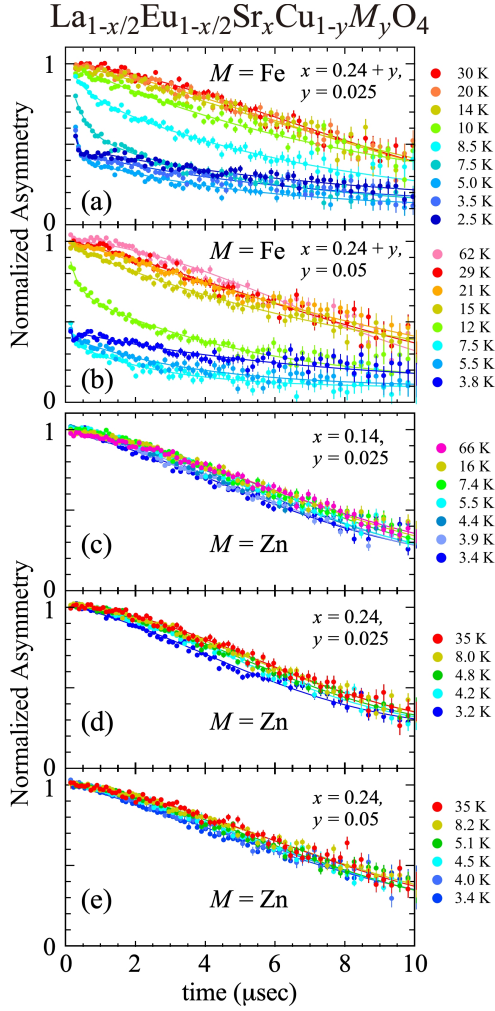


FIG. 3. (Color online) μ SR time spectra at zero-field for $\text{La}_{1-x/2}\text{Eu}_{1-x/2}\text{Sr}_x\text{Cu}_{1-y}\text{M}_y\text{O}_4$ with $(M, x, y) =$ (a) (Fe, 0.265, 0.025), (b) (Fe, 0.29, 0.05), (c) (Zn, 0.24, 0.025), (d) (Zn, 0.24, 0.05), and (e) (Zn, 0.14, 0.025).

~ 60 K has been reported for the pristine OA LESCO with $0.14 \leq x \leq 0.24$ [25]. This thermal evolution of the spectra in Fe-LESCO means the inducement of the magnetic state by Fe-substitution. By contrast, Gaussian-shaped spectra remain at ~ 3 K in Zn-LESCO, even with $y = 0.05$, indicating the absence of static magnetism. Thus, as suggested by the susceptibility measurements, the magnetic and non-magnetic ground states are realized by respective Fe and Zn substitution into LESCO with $x = 0.24$.

To evaluate the magnetic volume fraction (V_m), internal magnetic field at the muon stopping site (B_{int}), and magnetic ordering temperature, we analyzed the μ SR time spectra using the following functions.

$$A(t) = A_0 e^{-\lambda_0 t} G(\Delta, t) + A_1 e^{-\lambda_1 t} + A_2 e^{-\lambda_2 t} \cos(\gamma_\mu B_{\text{int}} t), \quad (1)$$

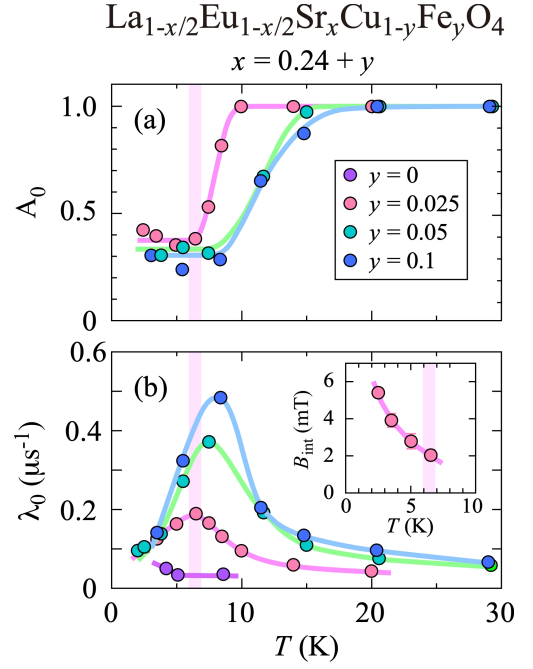


FIG. 4. (Color online) The temperature dependence of (a) initial asymmetry A_0 and (b) relaxation rate λ_0 estimated from the μ SR spectra in $\text{La}_{1-x/2}\text{Eu}_{1-x/2}\text{Sr}_x\text{Cu}_{1-y}\text{Fe}_y\text{O}_4$. λ_0 for $y = 0$ is obtained from the data in Ref. 25. The inset shows the temperature dependence of the internal field B_{int} for $y = 0.025$.

where

$$G(\Delta, t) = \frac{1}{3} + \frac{2}{3}(1 - \Delta^2 t^2)e^{-\frac{1}{2}\Delta^2 t^2}. \quad (2)$$

$G(\Delta, t)$ is the Kubo-Toyabe function, and Δ represents the distribution of the nuclear dipole field at muon site (full width at half maximum). The first term of Eq. 1 is the non-magnetic component exhibiting slow relaxation due to nuclear dipole fields randomly oriented at the muon site. The second and third terms represent the fast depolarization component due to slowly fluctuating electron spins and the magnetically ordered component, respectively. Here, A_0 , A_1 , and A_2 are the initial asymmetry at $t = 0$ corresponding to the fraction of the respective components. The total initial asymmetry, A_{tot} , is defined as $A_{\text{tot}} = A_0 + A_1 + A_2$ and normalized to be 1. Giving the magnetically ordered powder material, the $1/3$ of the spin direction of muons is parallel to the internal field. When the magnetic volume fraction is 100% and nuclear magnetic fields are negligible compared to that induced by electron spins, this $1/3$ component can be described as $A_0 = 1/3$ in Eq. (1). The second term is used when the rotation component is not observed. $A_1 + A_2 = \frac{2}{3}$ is a typical constraint for a powder sample and both A_1 and A_2 can have finite values for systems with inhomogeneous static magnetism.

Since, we confirmed the temperature-independent Δ

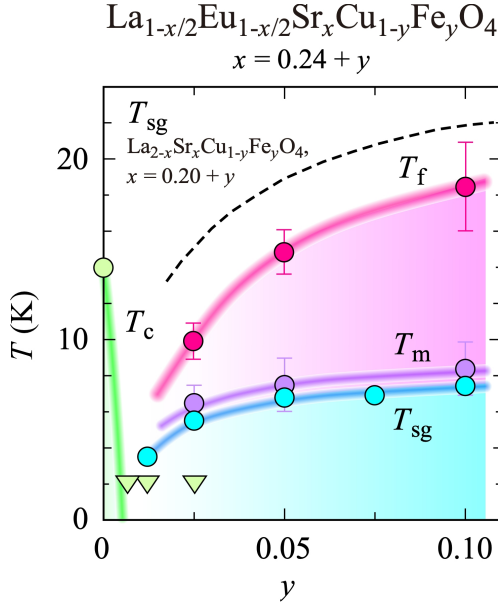


FIG. 5. (Color online) The Fe concentration dependencies of T_c (green circle and triangles), T_m (purple circles), T_{sg} (light blue circles), and T_f (pink circles) for $\text{La}_{1-x/2}\text{Eu}_{1-x/2}\text{Sr}_x\text{Cu}_{1-y}\text{Fe}_y\text{O}_4$ with $x = 0.24 + y$. T_m and T_{sg} are defined as the temperatures at which the temperature dependence of the relaxation rate for the non-magnetic component of the μSR time spectra and zero-field-cooled magnetic susceptibility respectively show the maximum. T_c (T_f) is evaluated from the results in the inset of Fig. 2(a) (Fig. 4(a)). The green triangles means that T_c is less than 2 K. The dashed line represents T_{sg} for overdoped $\text{La}_{2-x}\text{Sr}_x\text{Cu}_{1-y}\text{Fe}_y\text{O}_4$ with $x = 0.20 + y$ taken from Ref. 39

below 30 K, we fixed Δ as the averaged value for our analysis. λ_0 , λ_1 , and λ_2 are the relaxation rates. γ_μ and B_{int} indicate the gyromagnetic ratio of μ^+ ($2\pi \times 13.55$ kHz/G) and the average value of the internal magnetic field at the muon stopping site. This suggests that the Cu spins are partially ordered around the Fe ions, while most of the static magnetism corresponds to a spin glass state. Here, we assume a single muon stopping site, since the above equations can well reproduce the observed spectra.

Figures 4(a) and (b) show the temperature dependence of A_0 and λ_0 respectively for Fe-LESCO, with $x = 0.24 + y$ and $y = 0, 0.025, 0.050$, and 0.10 . The inset of Fig. 4 (b) shows B_{int} for $y = 0.025$. The results for pristine LESCO with $x = 0.24$ were adopted from Ref. 25. Upon cooling, A_0 for all the Fe-doped samples starts to decrease at 10 – 15 K. With further cooling, A_0 is reduced to $\sim 1/3$, corresponding to the value for the full magnetic volume fraction. Since the amount of doped Fe is 10% at most, the bulk magnetic order is not caused solely by Fe^{3+} spins, which are diluted on the CuO_2 planes.

The temperature for the maximum λ_0 (T_m) is comparable to the temperature at which A_0 reaches an almost constant value, and the weak oscillation component appears upon cooling. Therefore, the freezing of the spins

gradually occurs at lower temperatures. The increase in B_{int} below T_m indicates an increase in the moment size of the Cu spins in the ordered phase, although V_m is almost 100 %. However, the significant damping of the spectra suggests a rather short-range magnetic order with a broad distribution of the internal magnetic fields at the muon stopping sites, even at low temperatures. The same trend was obtained for the $y = 0.050$ and 0.10 samples. If the A_2 term is ignored, the behavior less than $2 \mu\text{s}$ cannot be reproduced in the Fe sample at the lowest temperature.

3. Magnetic state in LESCO with $x = 0.24$ ($p \sim 0.16$)

Fig. 5 summarizes the y -dependence of T_c , T_m and T_{sg} for $\text{La}_{1-x/2}\text{Eu}_{1-x/2}\text{Sr}_x\text{Cu}_{1-y}\text{Fe}_y\text{O}_4$ with $x = 0.24 + y$. T_{sg} for T -type Fe-LSCO with $x = 0.20 + y$ is shown by a dashed line as a reference [39]. The green triangles means that T_c is less than 2 K. The onset temperature for the development of V_m upon cooling (T_f) estimated from Fig. 4(a) is also plotted. T_m is slightly higher than T_{sg} at each concentration, and both T_m and T_{sg} increase weakly with increasing y . T_f is approximately double of T_m . This difference in the characteristic temperatures can be attributed to the experimental probes with different time windows to observe SG transition [34, 35, 39, 43, 44].

Here, we discuss the origin of the magnetic properties and electron states of LESCO by comparing them with T -type copper oxide. The results for Fe-LESCO are similar to those observed for OD Fe-LSCO in the following aspects: the emergence of bulk magnetic order by a partial Fe substitution, fast depolarization in the low temperature μSR spectra, and increase in T_m with increasing y . These characteristics are consistent with the presence of polarized itinerant spins in the SG state due to the Ruderman-Kittel-Kasuya-Yosida (RKKY) interaction in a metallic state, as indicated by the OD Fe-LSCO [37, 39] and OD Fe-substituted $\text{Bi}_{1.75}\text{Pb}_{0.35}\text{Sr}_{1.90}\text{CuO}_{4+\delta}$ [40, 45]. This implies that the randomly distributed magnetic moments on the CuO_2 planes cause fast depolarization in the μSR time spectra, and T_m tends to increase with an increase in the number of Fe ions, whose moments interact via itinerant carriers. Contrary to this, the strong damping of the μSR time spectra is different from the observation of a clear oscillation component for UD Fe-LSCO [36, 39], in which long-range magnetic and charge stripe orders coexist [41, 46].

As discussed in Refs. 35 and 39, better nesting conditions in OD samples enhance the spin polarization of the doped holes and stability of the magnetic order due to the RKKY interaction. In this context, the lower T_m in T^* -type Fe-LESCO than that in T -type Fe-LSCO with comparable p and y [36, 37, 39] suggests weaker RKKY interaction and nesting conditions in Fe-LESCO. The negligible Zn substitution effect on the static magnetism is similar to the results for OD Zn-LESCO, but

different from the enhancement of the magnetic order by Zn-substitution seen in UD LSCO [31–33]. Therefore, as is the case for the OD region of T -type LSCO, the itinerant spin nature is dominant in the present Fe-LESCO, and FL is most likely the ground state in the pristine T^* -type LESCO with $p \sim 0.16$.

C. Sr-concentration dependence of the magnetic state in $\text{La}_{1-x/2}\text{Eu}_{1-x/2}\text{Sr}_x\text{Cu}_{1-y}(\text{Fe}, \text{Zn})_y\text{O}_4$

1. Magnetic susceptibility and μSR measurements

Next, we examined the x -dependence of the magnetization for 5 % Fe-substituted LESCO with $0.19 \leq x \leq 0.34$ to investigate the extent to which the plausible FL state extends against x . As seen in Fig. 6, all the samples exhibit hysteresis in $\chi(T)$, indicating the inducement of the SG state by Fe substitution in a wide x range. Thus, T_{sg} is almost constant against x in the range between 0.19 and 0.34, as seen in the inset of Fig. 6. In contrast, in 5% Fe-LSCO (dashed line), T_{sg} increases rapidly from ~ 10 K for $x = 0.18$ to ~ 18 K for $x = 0.24$, and saturates above $x = 0.24$ [39]. The rapid change in T_{sg} seems to be associated with the cross-over of the ground state from the strongly correlated electronic state to the FL state [35, 39].

The constant value of T_{sg} in LESCO similar to the case of Fe-LSCO suggests the existence of the same electronic state, namely, the FL state in a broad x range. We note that evidence of successive magnetic transitions from the SG state followed by the spin-stripe ordered state upon cooling was reported for optimally doped and OD Fe-LESCO [37, 39]. That is, the $\chi(T)_{\text{ZFC}}$ and the temperature dependence of A_0 determined by μSR exhibits two local maxima and two peaks, respectively [37, 39]. However, in the present Fe-LESCO, no such behavior was observed for all the samples down to ~ 2 K, which is consistent with the absence of a stripe ordered state.

To further confirm the absence of a strongly correlated electronic state in T^* -type LESCO with lower p , we measured the 2.5% Zn-substitution effect on the magnetism in LESCO with $x = 0.14$ ($p \sim 0.09$, $T_c = 24.5$ K) by additional μSR experiments. In LSCO, a small amount of Zn substitution samples showed the stripe order in $p < 0.14$, but induces only weakly static magnetism in the FL state of the OD region [31–33]. Therefore, if a strongly correlated electronic state is present in the lower p region, the enhancement of static magnetism could be observed by Zn substitution. Fig. 3 (e) shows the thermal evolution of the observed μSR time spectra. The results are approximately identical to those of the temperature dependence for $x = 0.24$ ($p \sim 0.16$) and $y = 0.025$. The Gaussian-shaped spectra did not change with temperature, indicating the absence of static magnetism. Weak thermal evolution of the μSR time spectra with the remaining Gaussian-shaped depolarization was also observed in Zn-LESCO with $x = 0.14$ and $y = 0.05$

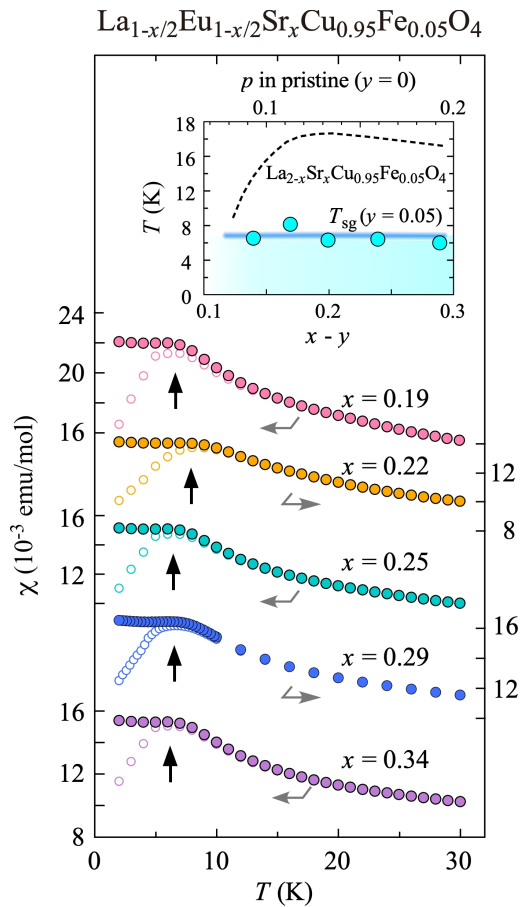


FIG. 6. (Color online) Temperature dependence of the magnetic susceptibility ($\chi(T)$) measured after FC and ZFC processes in a magnetic field of 500 Oe for $\text{La}_{1-x/2}\text{Eu}_{1-x/2}\text{Sr}_x\text{Cu}_{1-y}\text{Fe}_y\text{O}_4$ (Fe-LESCO) with $x = 0.19, 0.22, 0.25, 0.29, 0.34$ and $y = 0.05$. $\chi(T)$ are shifted for clear visualization. Arrows represent T_{sg} , where ZFC $\chi(T)$ is the maximum. The dashed line in the inset represents T_{sg} for $\text{La}_{2-x}\text{Sr}_x\text{Cu}_{0.95}\text{Fe}_{0.05}\text{O}_4$ taken from Ref. 39

and 0.10 (not shown here).

2. Relevance to T - and T' -type cuprates

In the present study, we obtained no evidence of cross-over of the electronic state against doping and successive magnetic order with decreasing temperature. Considering the above observations, we conclude that the SG-like state is most likely originated by RKKY interaction, and the FL state is realized in the present T^* -type LESCO with $x \geq 0.14$. Even when a stripe ordered phase exists, it would emerge in a more lightly doped region of the LESCO. Since the actual p value of 0.09 is reported for pristine LESCO with $x = 0.14$ [26], it can be concluded that the FL state is formed in the lower p region, contrary to that in T -type LESCO. The formation of the FL state with lower p can be attributed to

the smaller size of the charge-transfer gap (Δ_{CT}) in the parent T^* -type $RECuO_4$. From the optical conductivity measurements on various types of Cu-O single-layer networks, Tokura and co-workers clarified the smaller Δ_{CT} for RE_2CuO_4 with lower oxygen coordination [3]. Carrier doping into the system with smaller Δ_{CT} could induce the metallic state at lower p , because the charge transfer gap collapses easily with filling the in-gap state. Such a trend is reported for T' -type RE_2CuO_4 [1, 47–49] via Ce-substitution. The onset electron concentration for the emergence of superconductivity in $RE_2Ce_xCuO_4$ is lower in the system with a smaller Δ_{CT} in the parent compound. It is worth mentioning that Ce-free T' -type $La_{1.8}Eu_{0.2}CuO_4$, which has a large in-plane lattice constant (4.00 Å), exhibits superconductivity after adequate oxygen reduction annealing [11]. From the negative linear relation between Δ_{CT} and the in-plane lattice constant, $La_{1.8}Eu_{0.2}CuO_4$ is expected to have the smallest Δ_{CT} among the T' -type RE_2CuO_4 [4, 50]. Furthermore, the increase in T_c with lowering p in T^* -type LESCO is similar to the p -dependence of T_c in the hole-doped T' -type $La_{1.8-x}Eu_{0.2}(Sr, Ca)_xCuO_4$ [11, 28, 29]. This similarity suggests that the doping evolution of the electronic state in LESCO with five oxygen coordination is comparable to that in $La_{1.8-x}Eu_{0.2}(Sr, Ca)_xCuO_4$ with four coordination, than that in LSCO with six coordination. Of all the possibilities, the above discussion is the most likely candidate. Thus, our results suggest the importance of research on the lightly doped T^* -type cuprate for a unified understanding of the ground state in RE_2CuO_4 , and the mechanism of superconductivity from the viewpoint of Cu coordination.

IV. SUMMARY

We have investigated the magnetism in Fe- and Zn-substituted T^* -type LESCO by μ SR and magnetic susceptibility measurements for the first time to clarify the ground state in pristine LESCO. SG-like field-dependent behavior was observed in the temperature dependence of the magnetic susceptibility $\chi(T)$ in

Fe-LESCO. Using μ SR measurements, we confirmed the existence of bulk magnetic order in all Fe-LESCO samples, and a slight increase in the magnetic ordering temperature with Fe substitution. These results are quantitatively similar to the observation in OD T -type Fe-LSCO, for which the RKKY interaction was discussed as the origin of the magnetic order. Contrary to this, in Zn-LESCO, the paramagnetic behavior in $\chi(T)$ with no magnetic order was observed. All of these element substitution effects are consistent with those found in the OD LSCO [37, 39], suggesting that the FL ground state is realized in pristine OD LESCO from a lower p upon doping, compared to that in T -type LSCO. The existence of the FL state in the lower p region is possibly associated with the smaller size of the charge transfer gap in the T^* -type LESCO than in the T -type LSCO, owing to the lower number of oxygen coordinations. Our result suggests that the local crystal structure around the CuO_2 plane has a strong influence on the size of the charge transfer gap and plays a vital role in the mechanism of superconductivity in T^* -type LESCO.

ACKNOWLEDGEMENTS

We thank T. Adachi, Y. Koike, and Y. Miyazaki for fruitful discussions and appreciate T. Noji and T. Kawamata for their help in sample preparation. The μ SR experiments at the Materials and Life Science Experimental Facility of J-PARC (Proposal Nos. 2015MP001, 2018B0324, and 2019B0290) and at the RIKEN-RAL Muon Facility in the Rutherford Appleton Laboratory (Proposal No. RB1970107) were performed under user programs. We thank the J-PARC and the RIKEN-RAL staff for their technical support during the experiments. This work was partially supported by the IMSS Multiprobe Research Project, and M.F. and T.T. are supported by Grant-in-Aid for Scientific Research (A) (16H02125) and for Young Scientists(Start-up) (19K23417), respectively.

* taka.taniguchi@imr.tohoku.ac.jp

† Present address: Nuclear Structure Research Group, RIKEN Nishina Center for Accelerator-Based Science, RIKEN, Wako, Saitama 351-0198, Japan

‡ fujita@imr.tohoku.ac.jp

- [1] Y. Krockenberger, B. Eleazer, H. Irie, H. Yamamoto, J. Phys. Soc. Jpn. **83**, 114602 (2014).
- [2] T. Adachi, T. Kawamata, and Y. Koike, Condens. Matter **2**, 23 (2017).
- [3] Y. Tokura, S. Koshihara, T. Arima, H. Takagi, S. Ishibashi, T. Ido, S. Uchida, Phys. Rev. B **41**, 11657 (1990).

- [4] T. Arima, T. Kikuchi, M. Kasuya, S. Koshihara, Y. Tokura, T. Ido, S. Uchida, Phys. Rev. B **44**, 917 (1991).
- [5] S. Uchida, T. Ido, H. Takagi, T. Arima, Y. Tokura, S. Tajima, Phys. Rev. B **43** (1991) 7942.
- [6] Y. Onose, Y. Taguchi, K. Ishizaka, and Y. Tokura Phys. Rev. B **69** (2004) 024504.
- [7] A. Tsukada, Y. Krockenberger, M. Noda, H. Yamamoto, D. Manske, L. Alff, and M. Naito, Solid State Commun. **133**, 427 (2005).
- [8] O. Matsumoto, A. Utsuki, A. Tsukada, H. Yamamoto, T. Manabe, and M. Naito, Physica C **469**, 924 (2009).
- [9] O. Matsumoto, A. Utsuki, A. Tsukada, H. Yamamoto, T. Manabe, M. Naito, Phys. Rev. B **79**, 100508(R) (2009)

- [10] S. Asai, S. Ueda, and M. Naito, *Physica C* **471**, 682 (2011).
- [11] T. Takamatsu, M. Kato, T. Noji, and Y. Koike, *Appl. Phys. Express* **5**, 073101 (2012).
- [12] S. W. Jang, H. Sakakibara, H. Kino, T. Kotani, Kazuhiko K., and M. J. Han, *Scientific Reports* **6**, 33397 (2016).
- [13] P. G. Radaelli, J. D. Jorgensen, A. J. Schultz, J. L. Peng, R. L. Greene, *Phys. Rev. B* **49**, 15322 (1994).
- [14] X. Q. Xu, S. N. Mao, W. Jiang, J. L. Peng, R. L. Greene, *Phys. Rev. B* **53**, 871 (1996).
- [15] A. J. Schultz, J. D. Jorgensen, J. L. Peng, R. L. Greene, *Phys. Rev. B* **53**, 5157 (1996).
- [16] Y. Krockenberger, H. Irie, O. Matsumoto, K. Yamagami, M. Mitsuhashi, A. Tsukada, M. Naito, and H. Yamamoto, *Scientific Reports* **3**, 2235 (2013).
- [17] J. Akimitsu, S. Suzuki, M. Watanabe, and H. Sawa, *Jpn. J. Appl. Phys.* **27**, L1859 (1989).
- [18] H. Sawa, S. Suzuki, M. Watanabe, J. Akimitsu, H. Matsumura, H. Watabe, S. Uchida, K. Kokusho, H. Asano, F. Izumi, and E. Takayama-Muromachi, *Nature* **337**, 347 (1989).
- [19] K. M. Kojima, Y. Krockenberger, I. Yamauchi, M. Miyazaki, M. Hiraishi, A. Koda, R. Kadono, R. Kumai, H. Yamamoto, A. Ikeda, M. Naito, *Phys. Rev. B* **89**, 180508(R) (2014).
- [20] T. Adachi, Y. Mori, A. Takahashi, M. Kato, T. Nishizaki, T. Sasaki, N. Kobayashi and Y. Koike, *J. Phys. Soc. Jpn.* **82**, 063713 (2013).
- [21] T. Kawamata, K. Ohashi, T. Takamatsu, T. Adachi, M. Kato, I. Watanabe, and Y. Koike, *J. Phys. Soc. Jpn.* **87**, 094717 (2018).
- [22] S.-W. Cheong, Z. Fisk, J.D. Thompson, and R. B. Schwarz, *Physica C* **159**, 407 (1989).
- [23] Z. Fisk, S.-W. Cheong, J. D. Thompson, M. F. Hundley, R. B. Schwarz, and G. H. Kwei, *Physica C* **162-164**, 1681 (1989).
- [24] M. Fujita, K. M. Suzuki, S. Asano, A. Koda, H. Okabe, and R. Kadono, *JPS Conf. Proc.* **21**, 011026 (2018).
- [25] S. Asano, K. M. Suzuki, K. Kudo, I. Watanabe, A. Koda, R. Kadono, T. Noji, Y. Koike, T. Taniguchi, S. Kitagawa, K. Ishida, M. Fujita, *J. Phys. Soc. Jpn.* **88**, 084709 (2019).
- [26] S. Asano, K. Ishii, K. Yamagami, J. Miyawaki, Y. Harada, M. Fujita, *J. Phys. Soc. Jpn.* **89**, 075002 (2020).
- [27] H. Takagi, S. Uchida, and Y. Tokura, *Phys. Rev. Lett.* **62**, 1197 (1989).
- [28] T. Takamatsu, M. Kato, T. Noji, Y. Koike, *Phys. Procedia* **58**, 46 (2014).
- [29] T. Sunohara, T. Kawamata, K. Shiosaka, T. Takamatsu, T. Noji, M. Kato, and Yoji Koike, *J. Phys. Soc. Jpn.* **89**, 014701 (2020).
- [30] A. V. Balatsky, I. Vekhter, and Jian-Xin Zhu, *Rev. Mod. Phys.* **78**, 373 (2006), and references therein.
- [31] T. Adachi, S. Yairi, K. Takahashi, Y. Koike, I. Watanabe, K. Nagamine, *Phys. Rev. B* **69**, 184507 (2004).
- [32] Risdiana, T. Adachi, N. Oki, S. Yairi, Y. Tanabe, K. Omori, Y. Koike, T. Suzuki, I. Watanabe, A. Koda, W. Higemoto, *Phys. Rev. B* **77**, 054516 (2008).
- [33] T. Adachi, N. Oki, Risdiana, S. Yairi, Y. Koike, I. Watanabe, *Phys. Rev. B* **78**, 134515 (2008).
- [34] M. Fujita, M. Enoki, K. Yamada, *J. Phys. Chem. Solids* **69**, 3167 (2008).
- [35] R.-H. He, M. Fujita, M. Enoki, M. Hashimoto, S. Iikubo, S.-K. Mo, H. Yao, T. Adachi, Y. Koike, Z. Hussain, Z.-X. Shen, K. Yamada, *Phys. Rev. Lett.* **107**, 127002 (2011).
- [36] K. Suzuki, T. Adachi, Y. Tanabe, H. Sato, Risdiana, Y. Ishii, T. Suzuki, I. Watanabe, Y. Koike, *Phys. Procedia* **30**, 275 (2012).
- [37] K. M. Suzuki, T. Adachi, Y. Tanabe, H. Sato, Y. Koike, Risdiana, Y. Ishii, T. Suzuki, and I. Watanabe *Phys. Rev. B* **86**, 014522 (2012).
- [38] M. Z. Cieplak, A. Sienkiewicz, F. Mila, S. Guha, G. Xiao, J. Q. Xiao, C. L. Chien, *Phys. Rev. B* **48**, 4019 (1993).
- [39] K. M. Suzuki, T. Adachi, H. Sato, I. Watanabe, and Y. Koike, *J. Phys. Soc. Jpn.* **85**, 124705 (2016).
- [40] H. Hiraka, Y. Hayashi, S. Wakimoto, M. Takeda, K. Kaku-rai, T. Adachi, Y. Koike, I. Yamada, M. Miyazaki, M. Hiraishi, S. Takeshita, A. Kohda, R. Kadono, J. M. Tranquada, and K. Yamada, *Phys. Rev. B* **81**, 144501 (2010).
- [41] M. Fujita, M. Enoki, S. Iikubo, K. Kudo, N. Kobayashi, K. Yamada, *arXiv: 0903.5391* (2009).
- [42] J. W. Martin, G. J. Russell, A. Hartmann, D. D. Cohen, *Phys. Rev. B*, **53**, 9412 (1996).
- [43] S. Wakimoto, S. Ueki, Y. Endoh, and K. Yamada, *Phys. Rev. B* **62**, 3547 (2000).
- [44] M. Enoki, M. Fujita, S. Iikubo, J. M. Tranquada, and K. Yamada, *J. Phys. Soc. Jpn.* **80**, SB026 (2011).
- [45] S. Wakimoto, H. Hiraka, K. Kudo, D. Okamoto, T. Nishizaki, K. Kakurai, T. Hong, A. Zheludev, J. M. Tranquada, N. Kobayashi, K. Yamada, *Phys. Rev. B* **82**, 064507 (2010).
- [46] M. Fujita, M. Enoki, S. Iikubo, K. Yamada, *J. Supercond. Nov. Magn.* **22**, 243 (2009).
- [47] M. Naito, S. Karimoto, A. Tsukada, *Supercond. Sci. Technol.* **15**, 1663 (2002).
- [48] M. Fujita, T. Kubo, S. Kuroshima, T. Uefuji, K. Kawashima, K. Yamada, I. Watanabe, and K. Nagamine, *Phys. Rev. B* **67**, 014514 (2003).
- [49] Y. Krockenberger, J. Kurian, A. Winkler, A. Tsukada, M. Naito, and L. Alff, *Phys. Rev. B* **77**, 060505(R) (2008).
- [50] S. Asano, K. Ishii, D. Matsumura, T. Tsuji, K. Kudo, T. Taniguchi, S. Saito, T. Sunohara, T. Kawamata, Y. Koike, M. Fujita, *arXiv:2005.10681*